

1 **Spatial variations of methane emission in a large shallow eutrophic lake in subtropical**
2 **climate**

3

4 Qitao Xiao¹, Mi Zhang^{1,*}, Zhenghua Hu¹, Yunqiu Gao¹, Cheng Hu¹, Cheng Liu¹, Shoudong
5 Liu¹, Zhen Zhang¹, Jiayu Zhao¹, Wei Xiao¹, X Lee^{1,2,*}

6

7 ¹Yale-NUIST Center on Atmospheric Environment, Nanjing University of Information
8 Science & Technology, Nanjing, China

9

10 ²School of Forestry and Environmental Studies, Yale University, New Haven, Connecticut
11 06511, USA

12

13 * Corresponding author

14 Dr. Xuhui Lee

15 E-mail: xuhui.lee@yale.edu

16

17 Dr. Mi Zhang

18 E-mail: zhangm.80@nuist.edu.cn

19

20 Key points

21

22 Methane flux showed large seasonal and spatial variations.

23

24 The highest fluxes were observed in a highly eutrophic zone and a shallow zone dominated
25 by submerged macrophytes.

26

27 The annual mean CH₄ flux in this large and shallow eutrophic lake was much lower than
28 suggested previously for lakes in China.

29 **Abstract**

30 Subtropical lakes are an important source of atmospheric methane (CH₄). This study aims to
31 investigate spatial variations of the CH₄ flux in Lake Taihu, a large (area 2400 km²) and
32 shallow (mean depth 1.9 m) eutrophic lake in Eastern China. The lake exhibited high spatial
33 variations in pollution level, macrophyte vegetation abundance, and algal growth. We
34 measured the diffusion CH₄ flux via the transfer coefficient method across the whole lake. In
35 addition, data obtained with the flux-gradient and the eddy-covariance methods were used in
36 conjunction with the data on the diffusion flux to estimate the contribution by ebullition.
37 Results from three years' measurements indicate high spatial variabilities in the diffusion CH₄
38 flux. The spatial pattern of the diffusion CH₄ emission was correlated with water clarity, and
39 dissolved oxygen concentration, and with the spatial distributions of algal and submerged
40 vegetation. In comparison to the transfer coefficient method, the eddy covariance and the
41 flux-gradient method observed a lake CH₄ flux that was 3.39 ± 0.58 (mean \pm one standard
42 deviation) and 1.95 ± 0.36 times higher in an open-water eutrophic zone and in a habitat of
43 submerged macrophytes, respectively. The result implied an average of 71% and 49%
44 ebullition contribution to the total CH₄ flux in the two zones. The annual mean diffusion CH₄
45 flux of the whole lake was $0.54 \pm 0.30 \text{ g m}^{-2} \text{ year}^{-1}$. Our CH₄ emission data suggest that the
46 average CH₄ emission reported previously for lakes in Eastern China was overestimated.

47

48 **Key words:** Lake Taihu; CH₄ flux; Spatial pattern; Temporal variation

49 **1 Introduction**

50 Lakes occupy only 3.7% (5×10^6 km²) of the global land area (Verpoorter *et al.*, 2014), but
51 play a disproportionately large part in the atmospheric methane (CH₄) budget (Bastviken *et*
52 *al.*, 2011). Lake CH₄ emissions vary strongly across latitude and climatic gradient, showing
53 higher emission intensity at a lower latitude and in a warmer climate (Bastviken *et al.*, 2004;
54 Marotta *et al.*, 2014). So far, only a few observational studies have been conducted in
55 subtropical lakes, located between 25° and 40° of latitude based on the Strahler climatic
56 classification (Xing *et al.*, 2005; Palma-Silva *et al.*, 2013; Musenze *et al.*, 2014; Sturm *et al.*,
57 2014; Hu *et al.*, 2015). About one-third of lakes are located in these latitudes, occupying a
58 total surface area of 1.7×10^6 km² (Verpoorter *et al.*, 2014). It is estimated that lakes located
59 in these latitudes release about 30% of the total freshwater CH₄ emission (Bastviken *et al.*,
60 2011).

61

62 Field studies show that the lake CH₄ flux may vary seasonally and spatially. Generally, the
63 flux is higher in the summer than in the winter due to higher water temperature (Xing *et al.*,
64 2005; Palma-Silva *et al.*, 2013). The spatial heterogeneity is associated with aquatic
65 vegetation serving as sources of substrate for CH₄ production (Wang *et al.*, 2006; Chen *et al.*,
66 2009) or transporting oxygen to sediment for CH₄ oxidation (Holzapfel-Pschorn *et al.*, 1986;
67 Fritz *et al.*, 2011), and with lake morphometry (area and depth; Bastviken *et al.*, 2004; Rasilo
68 *et al.*, 2015; Holgersson *et al.*, 2016), river discharge and sediment type (Natchimuthu *et al.*
69 2015; Wik *et al.*, 2016). Therefore, observing temporal and spatial patterns of CH₄ flux are
70 necessary to accurately estimate whole-lake CH₄ emissions.

71 Some studies indicate that lake nutrient status and aquatic vegetation can impact CH₄
72 production and emission. A study of boreal lakes in Quebec, Canada showed that
73 summertime diffusion CH₄ flux is positively correlated with lake nutrient status (Rasilo *et al.*,
74 2015). A long-term mesocosm experiment demonstrated that changes in the lake
75 eutrophication status play a larger role in the CH₄ flux trend than changes in temperature
76 (Davidson *et al.*, 2015). The aerenchyma tissues and hollow stems of emergent vascular
77 aquatic vegetation can act as conduits allowing massive CH₄ to bypass the aerobic zone and
78 escape to the atmosphere (e. g., Bouchard *et al.*, 2007; Carmichael *et al.*, 2014). The
79 emergent plant conduits also transport oxygen from the vast atmospheric source to the
80 rhizosphere, having the potential to enhance CH₄ oxidation (Holzapfel-Pschorn *et al.*, 1986;
81 Fritz *et al.*, 2011). In the case of submerged vegetation, the source of oxygen is mostly
82 photosynthesis (e. g., Sorrell and Dromgoole, 1987), which may have a limited effect on CH₄
83 oxidation in the rhizosphere. At the end of the growing season, the dead submerged
84 vegetation accumulates at the lake bottom, supplying substrates for CH₄ production, which
85 may result in increased CH₄ emission. The role of submerged vegetation on the lake CH₄ flux
86 is not well understood.

87
88 Ebullition is an important pathway of the lake CH₄ flux. The CH₄ produced in the lake
89 sediment can form bubbles easily because of low solubility of CH₄ in water. These air
90 bubbles rise to the water surface much more rapidly than the diffusion process, allowing the
91 trapped CH₄ to escape oxidation. It is estimated that ebullition emission accounts for 40% to
92 60% of the lake CH₄ flux globally (Bastviken *et al.*, 2004) and 60% to 99% of the lake CH₄

93 flux in subtropical climates (Sturm *et al.*, 2014). Moreover, a survey of global lake data
94 revealed that ebullition occurs at 25 to 80% of the measurement sites in shallow water (depth
95 less than 4 m) and only 10% in deeper water (depth greater than 4 m; Bastviken *et al.*, 2004)
96 based on the chamber method. This depth dependence is explained by a lower water
97 hydrostatic pressure and a shorter transport pathway in shallower lakes (e. g., Joyce and
98 Jewell, 2003; DelSontro *et al.*, 2011). Wik *et al.* (2011; 2013) showed that ebullition
99 dominates the lake CH₄ emission but with large uncertainties due to high spatio-temporal
100 variabilities. More simultaneous measurements of diffusion and ebullition flux, especially in
101 large lakes, are needed to improve the assessment of the global lake CH₄ budget.

103 Our study site is Lake Taihu, a large shallow eutrophic lake in China. The specific objectives
104 of this study are: (1) to characterize within-lake and temporal variations of the CH₄ flux in the
105 lake, using observations made in open water zones and zones inhabited by submerged
106 macrophytes, (2) to investigate the relationships between biological, chemical and physical
107 factors and the observed flux variabilities, and (3) to compare the CH₄ flux of this lake with
108 the CH₄ fluxes reported for other lakes in China.

110 **2 Material and methods**

111 **2.1 Study site**

112 The measurements were made in Lake Taihu (30°05' to 32°08' N, 119°08' to 121°55' E) in
113 Eastern China. Lake Taihu has a surface area of 2400 km², a length of 70 km (from north to
114 south) and a width of 60 km (from east to west), a maximum depth of 3.3 m, and a mean

depth of 1.9 m (Qin *et al.*, 2007). The lake catchment area is 36500 km². The lake has a complex river network and is surrounded by several large cities (Qin *et al.*, 2007). The northern and western portions of the lake experience severe eutrophication due to pollution discharge via inflow rivers. Submerged vegetation was found in the cleaner eastern portion of the lake.

The lake is divided into seven zones according to vegetation distribution, eutrophic status, and wind-current interactions (Figure 1). *Meiliang Bay* is eutrophic due to pollution and organic matter discharge of two inflowing rivers; *Gonghu Bay* receives river discharge from Wuxi and Suzhou and is the intake of urban water, with half of the area inhabited by emergent aquatic vegetation. It is also the estuary of Wangyu River which is the main channel for water transfer between Yangtze River and Lake Taihu; The *Northwest Zone* is hyper-eutrophic due to pollution discharged by urban and agricultural runoffs; Water in the *Central Zone* is relatively clean and has low photosynthetic activity; The *East Zone* is the main outlet of the lake and is dominated by submerged vegetation; The *Southwest Zone* is connected to three large inflowing rivers and is a transitional region between phytoplankton dominance and submerged vegetation dominance; *Dongtaihu Bay* is a shallow bay used for aquaculture and is inhabited by submerged vegetation (Qin *et al.*, 2007; Hu *et al.*, 2011; Lee *et al.*, 2014). The lake was deepest in the Central Zone (Figure 2f, about 3 m deep) and shallowest in Dongtaihu Bay (about 1.3 m deep). The total phosphorous and nitrogen concentrations in the seven zones are given in Table S1 in the Supporting Information.

This study was supported by micrometeorological measurements at five sites in the lake (MLW, DPK, BFG, XLS, and PTS) and at one land site (DS; Figure 1). The five lake sites are located in five of the lake zones described above, and water samples at these locations were collected for measuring the diffusion CH₄ flux. Two of the micrometeorological sites (MLW and BFG) were equipped with instruments to measure the lake-air flux of CH₄ in-situ, as described below. Wind and temperature measurements at the lake sites were used to calculate the transfer coefficient and to determine if spatial variability in the CH₄ flux was correlated with these micrometeorological variables.

2.2 Measurements of the CH₄ flux

Measurement of the CH₄ flux in a large lake is challenging. Each of the available measurement techniques has its own advantages and disadvantages (Schubert *et al.*, 2012). The eddy covariance method (Peltola *et al.*, 2013; Podgrajsek *et al.*, 2014) and the flux-gradient method (Xiao *et al.*, 2014) measure the lake CH₄ flux in-situ and continuously, but they can only be deployed at a limited number of sites because of cost, accessibility and power requirement. The transfer coefficient method is much more versatile, allowing measurement at multiple sites and in remote fields. This method can measure fluxes below the detection limit of the micrometeorological methods, but cannot measure the ebullition flux because water samples collected near the surface are generally free of air bubbles. Here both sets of measurement techniques were deployed to investigate the CH₄ flux in Lake Taihu. The transfer coefficient method was used to quantify the diffusion flux at multiple points across the lake and in different seasons of the year. The contribution of ebullition was

determined by comparing the flux measured with the transfer coefficient method against the total flux measured with the micrometeorological flux-gradient and the eddy-covariance method. The flux-gradient instrument used here was free of density effects (Xiao *et al.*, 2014) but because of high power consumption it was deployed at a site near the shoreline (MLW) where there was A/C power supply. The eddy covariance instrument was deployed at a more remote lake site (BFG) and was powered by solar panels.

2.2.1 CH₄ lake surveys

We collected water samples from the lake to determine the dissolved CH₄ concentration. At MLW, the eddy covariance site near the north shore, sample collection occurred daily at midday since 2011. From August 2011 to July 2013, diel sampling was also conducted at the site to investigate possible diel variations of the CH₄ flux. During this period, water samples were collected every three hours for three consecutive days in each month. At the other remote lake sites (DPK, BFG, XLS, and PTS), sampling took place at every site visit at irregular intervals. A whole-lake survey was conducted once per season, in February, May, August and November, during which time one water sample was collected at each of the 29 spatial sampling locations distributed across the whole lake (Figure 1). Each whole-lake survey was completed between 9:00 and 16:00 local time in two consecutive days.

Bubble-free lake water was collected at the 20-cm depth below the lake surface using a 600 mL homemade sampler, with a 3-cm wide opening at the top sealed with a rubber cork. The cork was removed from the opening by a remote controller when the sampler reached the

desired depth, allowing water to enter the sampler, and was put back in the opening to seal the sampler after it was full. The water was then poured quickly into a 300-mL glass bottle, with the excess water overflowing out of the bottle. (The time of exposure to ambient air during this transfer process was about 20 seconds.) The bottle was immediately capped without headspace using a butyl rubber stopper. Both, the sampler and glass bottle had been washed with local bubble-free lake water before collection.

The water samples collected at the MLW site were stored in a refrigerator at 4 °C for one to two weeks before being sent to our laboratory for analysis. Water samples collected during the lake surveys were saved in ice-chilled coolers and were analyzed within 48 hours after the collection. Laboratory tests indicate that the influence of storage time on the dissolved CH₄ concentration was negligible (Supplementary Figure S1).

In order to determine the concentration of CH₄ dissolved in the water samples, ultra-high purity N₂ gas (99.999%) was injected into the glass bottle to create a 100-mL headspace. The N₂ gas entered the bottle via a syringe inserted in the rubber stopper at a slight positive pressure of 50 hPa, and 100-mL of water was pushed out of the bottle via a second syringe inserted in the stopper. The remaining water was not exposed to room air during this process. The fraction of airspace (0.33) was lower than those (0.4 to 0.5) reported by Striegl *et al.* (2012) and Crawford *et al.* (2013). The glass bottle was then shaken vigorously for 5 minutes to allow the dissolved CH₄ gas to reach equilibrium with the headspace. A small air sample (20 mL) was drawn from the headspace using a syringe with a three-way stopcock and

injected into a gas chromatograph (Model Agilent GC6890N, Agilent Co., CA, USA) equipped with a flame ionization detector for CH₄ detection. The dissolved CH₄ concentration in the in-situ surface water was calculated according to a temperature-dependent Henry's law constant and accounted for CH₄ in the headspace and in the water (Johnson *et al.*, 1990). A laboratory test showed that the calculated in-situ concentration was not sensitive to variations in the headspace fraction (Supplementary Figure S2).

2.2.2 The transfer coefficient method

The diffusive CH₄ flux ($F_{m,d}$, mmol m⁻² d⁻¹) at the water-air interface was calculated using the transfer coefficient method based on the bulk diffusion model, as:

$$F_{m,d} = k \times (C_w - C_{eq}) \quad (1)$$

where k is the gas transfer coefficient (m d⁻¹), C_w is the CH₄ concentration (mmol m⁻³) dissolved in the surface water (at the depth of 20-cm) and measured by gas chromatography, and C_{eq} is the gas concentration in water that is in equilibrium with the atmosphere at the in-situ temperature. The gas transfer coefficient k is dependent on wind speed and is normalized to a Schmidt number of 600 (Cole and Caraco, 1998). The wind speed was measured at the PTS eddy covariance site located in the lake center.

The results presented in the main text below were based on the k values obtained from the model described by Cole and Caraco (1998). Several recent formulations consider both wind shear and waterside convection (e. g., MacIntyre *et al.*, 2010). We also computed the

diffusion flux using the models given by Read *et al.* (2012), Heiskanen *et al.* (2014), and Podgrajsek *et al.* (2015) for the transfer coefficient k . Details of these models are described in the Online Supplementary Information.

2.2.3 The flux-gradient and the eddy covariance method

These two micrometeorological techniques measure the CH₄ flux in-situ and continuously. The flux-gradient method determines the flux using an eddy diffusivity model and measurement of the vertical CH₄ concentration gradient above lake surface. The eddy covariance method determines the flux by measurement of the vertical wind speed and the CH₄ density above the water surface at high frequencies.

Even though measurements of the energy, the CO₂ and the H₂O fluxes were made at all the eddy covariance sites, only two of the sites, the MLW and the BFG site, were equipped with micrometeorological CH₄ flux instruments. At MLW, the total (diffusion plus ebullition) flux across the water-air interface was measured with the flux-gradient method, as

$$F_m = -0.55 \rho_a K \frac{r_2 - r_1}{z_2 - z_1} \quad (2)$$

where 0.55 is a unit conversion constant for CH₄, ρ_a is air density, r_1 and r_2 are the atmospheric CH₄ mixing ratio in reference to dry air at height z_1 and z_2 above the water surface, respectively, and K is the eddy diffusivity calculated with the Monin-Obukhov similarity functions using the aerodynamic method. A more detailed description about the method is given by Xiao *et al.* (2014). The gas measurement heights were approximately 1.1 and 3.5 m above the water surface. The concentration measurement was made sequentially

with a closed-path CH₄ analyzer (Model G1301, Picarro Inc., CA, USA). The CH₄ flux was determined at half-hourly intervals.

At BFG, a site dominated by submerged macrophytes (*Hydrilla verticillata* and *Potamogeton malaianus*), an eddy covariance system was used to measure the total water-air CH₄ flux, as

$$F_m = \overline{w'c'} \quad (3)$$

where w' and c' are fluctuations in the vertical wind speed and in the CH₄ density, respectively, and the overbar denotes block averaging. The system consisted of a three-dimensional sonic anemometer (Model CSAT3, Campbell Scientific Inc., Logan, UT, USA) for measuring three dimensional wind speeds, an open-path infrared gas analyzer (Model EC150, Campbell Scientific Inc.) for measuring atmospheric H₂O and CO₂ concentrations, and an open-path CH₄ gas analyzer (Model Li-7700, LI-COR Inc., Lincoln, NE, USA) for measuring the CH₄ concentration. These quantities were sampled at 10 Hz and the flux was computed at half-hourly intervals. Density effects were corrected according to the WPL theory, a theory named after the authors Webb, Pearman and Leuning (Webb *et al.*, 1980; Lee and Massman, 2011).

At these two sites, the peak contribution to the flux footprint was located at a distance of about 200 m from the flux tower in neutral stability (Xiao *et al.*, 2013). The energy balance closure was about 80% (Wang *et al.*, 2014). Of the micrometeorological observations, only those that coincided with lake water samplings were chosen for the purpose of methods comparison. Additionally, for the MLW site, the selected observations also satisfied good

fetch conditions (wind direction 180° - 270°; Xiao *et al.*, 2014). In other words, data collected during land breezes were excluded to avoid land influences. In the case of BFG, the distance to the nearest land is about 4 km which is much greater than the fetch required for eddy covariance application, so the measurement represented the lake flux under both land and lake breezes conditions and no wind direction screening was applied.

2.3 Ancillary data

Micrometeorological measurements at the five lake sites included wind speed and direction, water temperature, air temperature, relative humidity, and four-way net radiation components (Lee *et al.*, 2014). Four-way net radiation components were measured at a height of 2 m above the water surface.

Water physical, biological and chemical properties [water temperature, pH, turbidity (Turb), water clarity (given by Secchi disc depth), specific conductance (Spc), chlorophyll-a concentration (Chl-a), and dissolved oxygen concentration (DO)] were measured in-situ with a multi-parameter probe (YSI 650MDS, YSI Inc., Yellow Springs, OH, USA) at 20-cm depth and timed with water sample collections. The Chl-a measurement was checked against a zero solution prior to each field survey but was not compared to solutions of known Chl-a concentration. The Chl-a measurement was used only as a proxy for the true value in the analysis of spatial correlation described below. Other YSI parameters were calibrated monthly using the protocol recommended by the manufacturer.

Normalized Difference Vegetation Index (NDVI) is high when there are macrophytes and was used as a proxy for algal and macrophyte biomass in the surface water (e. g., Sawaya *et al.*, 2003; Cho and Lu, 2010). NDVI is a normalized difference in reflectance between the near-infrared and the red waveband. Because green biomass (algae and aquatic plants) has much higher reflectance in the near-infrared waveband than in the red waveband, a water pixel that has a high level of green biomass at or near the surface will have a high NDVI value. The NDVI product was based on the MODIS sensor on NASA's Terra platform, which has a time resolution of 16 days and a spatial resolution of 250 m. The actual time resolution after removing invalid data varies between 16 to 32 days.

2.4 Data analysis

Single variable regression and multilinear stepwise regression were used to investigate the relationships between environmental variables and the diffusion CH₄ flux. The variance inflation factor (VIF) was used to determine if multicollinearity could be omitted in the multiple linear regression. When VIF was greater than 5, any of the predictors was eliminated to reduce the multicollinearity (Manns *et al.*, 2013). According to the Akaike information criterion (AIC), the equation with the lowest AIC value was the best. The effect of each explanatory variable on multiple regression equation was assessed. In the analysis of spatial variability, measurements made at each of the 29 sampling sites (Figure 1) were first averaged over the three-year measurement period, and spatial correlation analysis was performed on these time-averaged quantities. In the analysis of temporal variability, zonal mean flux and environmental variables were used. The zonal mean value was calculated for

each lake survey using measurements made at the sites within that zone. The number of data points in these temporal correlation analyses was 12, each corresponding to one lake survey over the course of the three-year sampling period.

The fractional contribution of ebullition to the total CH_4 flux at two sites (MLW and BFG) was computed as the ratio of the ebullition flux, which was calculated as the difference between the micrometeorological flux and the diffusion flux, to the micrometeorological flux which is equivalent to the total flux.

2.5 Zonal and whole-lake fluxes

The diffusion flux for each lake zone was computed as the mean value of the flux using the spatial sampling locations in that zone. For Meiliang Bay, Gonghu Bay, the Central Zone, the East Zone, and Dongtaihu Bay, the zonal flux showed significant linear correlation with water temperature. To obtain the annual mean value for each zone, we established a linear regression equation between the diffusion flux and water temperature (Table 1), applied the equation to calculate the daily flux for the observation period (from January 1, 2012 to December 31, 2014) using the daily water temperature measured at BFG site (Figure 1), and averaged these daily values. The uncertainty of this annual mean diffusion flux was assessed with a Monte Carlo procedure assuming a normal distribution of errors in the regression coefficients. The standard deviation of the mean diffusion flux was based on a total of 10000 Monte Carlo ensemble members. For the Southwest Zone and the Northwest Zone, the correlation with temperature was statistically insignificant; their annual mean diffusion flux

was computed as the average of the data obtained from the seasonal surveys. The whole lake flux was computed as area-weighted mean of the zonal flux.

3 Results

3.1 Spatial variations of physical, biological and chemical factors

Water temperature of Lake Taihu is remarkably uniform. The spatial variability across the lake is less than 2 °C at hourly intervals (Deng *et al.*, 2013; Lee *et al.*, 2014) and less than 0.6 °C at monthly intervals (Wang *et al.*, 2014). At the annual intervals, the water temperature differences among the five micrometeorological lake sites were less than 0.4 °C (Figure 1). The annual mean water temperature at the 20-cm depth was 18.1, 17.9, and 17.8 °C at BFG for 2012, 2013 and 2014, respectively. The highest monthly mean was 31 °C (August 2013) and the lowest monthly mean was 3.9 °C (January 2013). Wind speed appeared quite uniform across the open water too. The annual mean wind speed at the 10 m height above the water surface were 2.96, 4.51, 4.45, 4.48, and 4.66 m s⁻¹, at MLW, DPK, BFG, XLS, and PTS, respectively (Figure 1). The wind speed at MLW was lower than at the other sites due to the sheltering effect of the local terrain.

In contrast to water temperature and wind speed, the biochemical properties displayed large spatial variations (Figure 2). The highest mean NDVI value (0.28) occurred in the East Zone and Dongtaihu Bay because of aquatic vegetation. Meiliang Bay and the Northwest Zone also showed relatively high NDVI values, indicating high algal abundance. The lowest DO and pH and the highest Chl-a were found in the Northwest Zone due to pollution discharge by

inflow rivers. The pH spatial variation was much larger than temporal variations over the spatial sampling interval (9:00 to 16:00 location time) (Supplementary Figure S3; Hu *et al.*, 2015). The water clarity index was highest in the East Zone and Dongtaihu Bay where submerged vegetation was abundant.

3.2 Temporal and spatial variations of the CH₄ diffusion flux

The CH₄ diffusion flux measured with the transfer coefficient method showed strong temporal variations at the five observation sites where frequent samplings took place (Figure 3). The highest CH₄ emission flux generally occurred in the summer, and the lowest flux always occurred in the winter. The average wintertime (January, February, and December) flux at MLW site ($0.033 \text{ mmol m}^{-2} \text{ d}^{-1}$) was about six times lower than the summer value ($0.213 \text{ mmol m}^{-2} \text{ d}^{-1}$). The mean CH₄ flux was 0.125 (MLW), 0.141 (BFG), 0.052 (DPK), 0.031(XLS), and $0.018 \text{ mmol m}^{-2} \text{ d}^{-1}$ (PTS). MLW is in the northern portion of Lake Taihu where algal growth was very severe, BFG is in a submerged vegetation habitat, and PTS is at the lake center (Figure 1). The mean dissolved CH₄ concentration was 132 (MLW), 130 (BFG), 51 (DPK), 27 (XLS), and 18 nmol L^{-1} (PTS) (Supplementary Figure S4).

Diel variations in the diffusion CH₄ flux were small at the MLW site (Figure S6). The CH₄ diffusion flux varied in a narrow range ($0.021\text{--}0.032 \text{ mmol m}^{-2} \text{ d}^{-1}$) over the 24 h cycle in the cold season (November to March). Averaged over the year, the daytime flux ($0.149 \pm 0.003 \text{ mmol m}^{-2} \text{ d}^{-1}$) was slightly lower than the nighttime flux ($0.156 \pm 0.022 \text{ mmol m}^{-2} \text{ d}^{-1}$; Figure S6).

The CH₄ diffusion flux shows very large spatial variations across the lake on the days of the spring and the summer lake surveys, ranging from 0.009 to 0.560 mmol m⁻² d⁻¹ in the spring, and from 0.020 to 0.507 mmol m⁻² d⁻¹ in the summer. The highest CH₄ flux occurred in Dongtaihu Bay and the East Zone, two regions without direct river nutrient inputs (Figure 1) but with high abundance of submerged macrophytes, where water was more clear and less deep than the other areas (Figure 2, panels e and f). The spatial variability was very weak on the days of the winter lake surveys, with the diffusion flux ranging from 0.006 to 0.107 mmol m⁻² d⁻¹ except for an isolated spot in the Northwest Zone where the flux reached 0.211 mmol m⁻² d⁻¹. The wintertime flux was very small (less than 0.08 mmol m⁻² d⁻¹) in the submerged macrophyte habitats (Figure 4d).

On an annual basis, Dongtaihu Bay, the East Zone, and the Northwest Zone were hot spots of CH₄ emission, followed by Meiliang Bay and Gonghu Bay (Figure 5). The lowest CH₄ emission occurred in the Central Zone.

3.3 Factors influencing the CH₄ flux variations

The whole-lake mean CH₄ diffusion flux increased linearly with water temperature, as shown in Figure 6, where each data point represents the spatial mean value of one whole-lake survey. The temporal CH₄ flux was poorly correlated with wind speed (the Pearson correlation coefficient $R = 0.50$, $n = 12$, $p = 0.09$). Temporal variations in water temperature explained 58% of the observed variance in the whole-lake flux ($R^2 = 0.58$, $n = 12$, $p < 0.01$).

401 The zonal mean diffusion flux exhibits different responses to water temperature (Table 1).

402 Temporal variations of the diffusion flux were highly correlated with water temperature for

403 the two macrophyte zones (the East Zone: $R = 0.81$, $p < 0.01$, $n = 12$; Dongtaihu Bay: $R =$

404 0.77 , $p < 0.01$, $n = 12$). However, the flux in the highly eutrophic West Zone fluctuated

405 around the mean value of $0.191 \text{ mmol m}^{-2} \text{ d}^{-1}$, showing poor correlation with water

406 temperature ($R = -0.10$, $p = 0.74$, $n = 12$).

407

408 The zonal flux temporal variations also depended on biochemical variables, some of which

409 displayed seasonal variations. The temporal variations in the CH_4 diffusion flux was

410 correlated with DO in Meiliang Bay ($R = -0.63$, $n = 12$, $p = 0.03$) and in the East Zone ($R =$

411 -0.83 , $n = 12$, $p < 0.01$), and with NDVI in the hyper eutrophic Northwest Zone ($R = 0.82$, $n =$

412 12 , $p < 0.01$) and in the East Zone ($R = 0.66$, $n = 12$, $p < 0.05$). However, the diffusion CH_4

413 flux did not show significant correlation with DO or NDVI in Dongtaihu Bay (DO: $p = 0.11$;

414 NDVI: $p = 0.06$). In this shallow submerged macrophytes zone, temperature and water depth

415 variations together explained 83% of the temporal variations in the observed CH_4 flux ($R^2 =$

416 0.83 , $n = 12$, $p < 0.01$).

417

418 Significant relationships were found between spatial variations of the diffusion flux and some

419 of the explanatory biochemical variables (Table 2, Figure 2). In this spatial correlation

420 analysis, each data point represents the mean value of whole experimental period

421 (2012-2014) for one of the 29 spatial sampling locations (Figure 1). The CH_4 diffusion flux

422 increased linearly with NDVI (Figure 7; $p < 0.001$), indicating that growth of algal and

aquatic vegetation could promote CH₄ emission. But the CH₄ diffusion flux decreased linearly with increasing dissolved oxygen concentration, pH, turbidity, and water depth, and increased with increasing water clarity (Table 2 and Figure 7). Correlations with chlorophyll concentration, specific conductance and oxidation reduction potential were not significant (Table 2). According to the Akaike Information Criterion (AIC), the best model to predict the CH₄ diffusion flux (mmol m⁻² d⁻¹) was that which contained water clarity (*c*, m), dissolved oxygen concentration (DO, mg L⁻¹), water depth (*d*, m), and NDVI. When one of these explanatory variables was removed, the AIC would go up. The multilinear stepwise regression function is

$$F_{m,d} = 0.184 c - 0.037 DO - 0.086 d + 0.355 NDVI + 0.552 \quad (4)$$

This regression model explained 78% of the observed spatial variability in the diffusion CH₄ flux ($R^2 = 0.78$, $p < 0.01$, $n = 29$). Some of explanatory biochemical variables were correlated (Supplementary Table S3). The variance inflation factor (VIF) values for the predictors in Equation (4) were lower than the threshold of 5 (Supplementary Table S4), showing that multicollinearity among these factors was negligible.

3.4 Diffusion flux and ebullition estimates

The mean diffusion CH₄ flux of whole lake was 0.092 ± 0.052 mmol m⁻² d⁻¹ or 0.54 ± 0.30 g m⁻² yr⁻¹ based on continuous measurements (Table 3). The highest diffusion CH₄ flux was in Dongtaihu Bay. These flux estimates were based on measurements made in the daytime. The diel sampling at MLW shows that the daytime flux was 4% lower than the whole-day flux (Figure S6), so the whole-lake flux reported here may have been underestimated by a similar

amount.

As explained in the Methods section, the annual mean flux was based on the application of a linear regression model for the zones where the correlation with temperature was significant. We also established an exponential regression equation, which might make more sense physically, to obtain the daily and then annual mean flux for these zones. The results are not sensitive to the model chosen (Table 3).

The CH₄ ebullition contribution was estimated based on the difference between diffusion flux and the total flux measured by the flux-gradient method and the eddy covariance method. At the MLW site, there were 41 half-hourly flux-gradient observations that took place under open-fetch conditions and coincided with the diffusive CH₄ measurement. The two measurements were correlated ($R = 0.41$, $p < 0.01$). The mean CH₄ flux of these observations was 0.707 and 0.199 mmol m⁻² d⁻¹ according to the flux-gradient method and the transfer coefficient method, respectively (Figure 8a). The regression slope (mean \pm 1 standard deviation) of the total flux versus the diffusion flux was 3.39 ± 0.58 , which was determined by the geometric mean functional regression. The result implied that the fractional contribution of ebullition to the total flux was 0.71 ± 0.06 .

At the BFG site, 11 valid eddy flux observations occurred at times of the dissolved CH₄ measurement (Figure 8b). The mean CH₄ flux was 0.319 and 0.185 mmol m⁻² d⁻¹ according to the eddy-covariance method and the transfer coefficient method, respectively. The regression

slope of the total flux versus the diffusion flux was 1.95 ± 0.36 . In this lake zone, the

fractional contribution of ebullition to the total flux was 0.49 ± 0.08 .

4 Discussion

4.1 Impact of eutrophic status

The large difference in the CH_4 flux between the algal bloom zones and the zones of low algal biomass supports the interpretation that eutrophic status plays a role in lake CH_4 emission. The Northwest Zone and Meiliang Bay were hyper-eutrophic due to high levels of nutrient discharges by inflow rivers (Qin *et al.*, 2007; Hu *et al.*, 2011; Supplementary Table S1). The mean diffusion flux was 0.191 ± 0.117 and $0.088 \pm 0.031 \text{ mmol m}^{-2} \text{ d}^{-1}$ in these two zones, respectively. For comparison, the mean diffusion flux was $0.025 \pm 0.015 \text{ mmol m}^{-2} \text{ d}^{-1}$ in the relatively clean Central Zone. High abundance of phytoplankton in the Northwest Zone and Meiliang Bay was indicated by the high NDVI and Chl-a levels (Figure 2a and d).

Because wind speed, water temperature, solar radiation, and sensible and latent heat fluxes show little spatial variations across the lake (Wang *et al.*, 2014), the contrast between the eutrophic zones and the Central zone can be interpreted as a consequence of different eutrophic conditions, rather than different micrometeorological conditions. Previous studies on the impact of eutrophication are based on measurements made at multiple lakes. Our results suggest that the impact can exist along the eutrophication gradient in a single lake.

In aquatic ecosystems, the majority of CH_4 is produced in the sediment by organic matter decomposition in anaerobic conditions. The net flux to the atmosphere is lower than the

production rate because some of the CH₄ is consumed by aerobic bacteria during the process of diffusion and transport (Segers, 1998; Bastviken *et al.*, 2008). The organic matter supply and dissolved oxygen concentration in the sediment are important factors that influence CH₄ production and the subsequent emission. High nutrient loading in eutrophic lakes not only increases autochthonous production, which then fuels CH₄ production, but also increases oxygen consumption, which suppresses CH₄ oxidation (Huttunen *et al.*, 2003). In this study, the lowest surface water DO was observed in the Northwest Zone (Figure 2b), the zone with the second highest diffusion CH₄ flux (Table 3). It is likely that DO was also low in the sediment pores in the zone, because DO shows virtually no vertical changes in the water column in Lake Taihu (Hu *et al.*, 2015). Our results show that DO was a variable that can explain some of the CH₄ flux spatial variations across the lake (Table 2; Equation 4). Although not low enough to limit CH₄ oxidation, the low DO levels were an indication of poor water quality and high nutrient load, which contributed to the high CH₄ emission. Additionally, co-variation might arise from the fact that oxygen flux and the diffusion CH₄ flux are both influenced by the piston velocity, namely the physical exchange rate.

Previous studies found that Chl-a is a good indicator of eutrophic influences on the CH₄ flux (Bastviken *et al.*, 2004; Rasilo *et al.*, 2015). In the present study, even though the highest Chl-a was found in the Northwest Zone with vast allochthonous nutrient input, the correlation between temporal variability of the CH₄ emission and Chl-a was insignificant in this zone ($R = -0.26, p = 0.45$). Some studies show that allochthonous nutrient input plays a larger role in lake CH₄ emission than the Chl-a level (Huttunen *et al.*, 2003; Ojala *et al.*, 2011). It is

possible that the influence of Chl-a on CH₄ flux may have been masked by the high nutrient loads and sediment inputs by river discharge (DelSontro *et al.*, 2011; Natchimuthu *et al.*, 2015). However, we cannot rule out that the poor temporal correlation with Chl-a was related to the fact that the Chl-a measurement was not calibrated to an absolute Chl-a standard (Section 2.3).

In comparison, a stronger correlation existed between temporal variations in the CH₄ diffusion flux and NDVI in the Northwest Zone ($R = 0.82$, $n = 12$, $p < 0.01$). It appears that NDVI, an indicator of algal abundance or nutrient input (DelSontro *et al.*, 2011), was a useful parameter for explaining the CH₄ emission variations in this eutrophic zone.

4.2 The role of submerged vegetation

The Chl-a spatial distribution showed that nutrient loading was the lowest in Dongtaihu Bay (Figure 2d). However, the CH₄ diffusion flux was the highest in this zone ($0.227 \text{ mmol m}^{-2} \text{ d}^{-1}$). The water was shallower in Dongtaihu Bay and in part of the East Zone than in the rest of the lake (Figure 2f), which encouraged growth of submerged vegetation (*Potamogeton malaianus* and *Hydrilla varticillata*) as indicated by the high NDVI values (Figure 2a). And the growth of macrophyte can influence the organic matter in the sediment (Wang *et al.*, 2006). The high CH₄ flux indicates that the submerged vegetation was an important substrate source that stimulated CH₄ production in these two zones (Ding *et al.*, 2005; Bridgham *et al.*, 2013; Carmichael *et al.*, 2014).

An alternative explanation for the high flux was the fact that these zones were shallow (mean depth 1.8 m). Indeed, water depth was highly correlated with spatial variations in the observed flux across the lake (Table 2). This correlation may have been enhanced by macrophyte vegetation and substrates in the sediment.

The CH₄ flux increased linearly with temperature in macrophyte zones (Table 1). The temporal variations in the diffusion CH₄ flux were correlated significantly with variations in the submerged vegetation biomass, approximated here by NDVI (East Zone: $R = 0.66$, $n = 12$, $p < 0.05$). But the CH₄ flux in the macrophyte zones was as low as in other zones during the wintertime (Figure 4d), suggesting that temperature rather than substrate availability was the limiting factor in CH₄ production in the cold season.

4.3 Temperature influences on CH₄ flux temporal variations

The temporal variations in the whole lake CH₄ diffusion flux significantly increased with water temperature (Figure 6). Temperature played a large role in determining the lake CH₄ emission of Lake Taihu, explaining 58% of the observed temporal variability in the CH₄ flux at the whole lake scale.

However, the role of temperature varied among the seven zones (Table 1). The most notable feature is the poor correlation for the Northwest Zone and the Southwest Zone. These two zones receive two thirds of the river runoff into the lake (Zhai *et al.*, 2010). The lack of temperature influence in these zones suggests that high nutrient inputs (Furlanetto *et al.*,

2012; Rasilo *et al.*, 2015) and high sediment loads (Natchimuthu *et al.*, 2015) may have confounded the direct effect of temperature on the CH₄ flux. Natchimuthu *et al.* (2015) observed higher CH₄ concentration in lake zones that receive stream water than their whole-lake mean concentration, and proposed that enhanced CH₄ production in sediments in these zones is a factor contributing to this difference. A long-term experiment shows that nutrient concentration outweighs temperature in determining lake CH₄ emission (Davidson *et al.*, 2015). In another related experiment in boreal lakes, the temperature dependency of the CH₄ flux decreases with increasing nutrient level (Rasilo *et al.*, 2015).

The CH₄ flux temperature dependency may offset the influence of water-side mixing at night. Podgrajsek *et al.* (2014) reported that stronger water-side mixing at night allows CH₄ to diffuse out of the water column more quickly than during the day at a shallow lake in central Sweden. On the other hand, lower production is expected at night due to lower temperatures than during the day. The weak CH₄ flux diel cycle at MLW (Figure S6) suggests that these two processes approximately offset one another at MLW.

4.4 CH₄ ebullition emission

In the present study, the ebullition flux accounted for a higher percent of the total flux in the eutrophic zone (mean value 71%, Figure 8a) than in the zone with submerged macrophytes (mean value 49%, Figure 8b). Because of relatively high amounts of submerged vegetation (peak biomass density 0.43 kg m⁻²; Gu *et al.*, 2005), Dongtaihu Bay and the East Zone, the two shallow water zones bear some resemblance to wetland ecosystems. In wetlands,

ebullition emission comprises only 13 to 48% of the total CH₄ flux (Gogo *et al.*, 2011; Maeck *et al.*, 2013; Crawford *et al.*, 2014). However, the difference in the ebullition contribution between MLW and BFG is not statistically significant ($p = 0.20$). Given the episodic nature of ebullition, the number of observations presented here ($n = 11$ at BFG and $n = 41$ at MLW) may be too small to draw a firm conclusion as to whether the submerged vegetation suppressed ebullition.

On the assumption that the ebullition fractional contribution measured at MLW was representative of the five open-water zones (Meiliang Bay, Gonghu Bay, Central Zone, Southwest Zone, and Northwest Zone) and that measured at BFG was representative of the two macrophyte zones (East Zone and Dongtaihu Bay), we estimated that the whole-lake mean ebullition flux was $0.99 \pm 0.27 \text{ g m}^{-2} \text{ yr}^{-1}$ and the total flux (diffusion plus ebullition) was $1.54 \text{ g m}^{-2} \text{ yr}^{-1}$. However, this whole-lake extrapolation should be viewed with caution. Our ebullition estimates are indirect and are based on the difference between two methods whose footprints are very different. Furthermore, ebullition is known to be highly sporadic both temporally and spatially (Wik *et al.*, 2011 and 2013). More temporal and spatial measurements in the lake are needed to address this issue.

4.5 Comparison of the annual mean CH₄ flux with other published studies

Based on the three years field measurement, the mean diffusion CH₄ flux of whole lake was $0.092 \pm 0.052 \text{ mmol m}^{-2} \text{ d}^{-1}$ or $0.54 \pm 0.30 \text{ g m}^{-2} \text{ yr}^{-1}$. The diffusion flux was much higher than that expected of the size-dependent scaling relationship given by Holgerson and

Raymond (2016). These authors showed that the dissolved CH₄ concentration and therefore the diffusion flux density decrease with increasing lake area. The smaller shoreline to surface area ratio in a larger lake contributes to the lower CH₄ diffusion flux because of the lower relative allochthonous carbon input. Extrapolating their relationship to 2400 km², the area of Lake Taihu, we obtained a much lower diffusion flux of 0.01 mmol m⁻² d⁻¹ than the measured value of 0.092 mmol m⁻² d⁻¹. One contributor to this anomalously high flux is that CH₄ emission in Lake Taihu was fueled by both allochthonous carbon input and in-situ production through algal photosynthesis and assimilation by the aquatic plants. In addition, higher gas transfer velocities in larger lakes (Read *et al.*, 2012) may also contribute to higher diffusion fluxes. The mean gas transfer velocity (converted to k_{600} , 1.23 m d⁻¹) in Lake Taihu was higher than the value of 1.15 m d⁻¹ recommended by Holgerson and Raymond (2016) for large lakes (> 100 km²). Rasilo *et al.* (2015) found that the warm season diffusion flux decreases with increasing lake area up to a threshold of ~100 km² for lakes in boreal Quebec; Lakes with area greater than this threshold seem to show a stable diffusion flux of 0.17 mmol m⁻² d⁻¹. These differences are a reminder that simple models based on lake physical characteristics alone may need to be constrained by local conditions to achieve improved performance.

It has been suggested that the CH₄ emission flux in Chinese lakes is much higher than in lakes elsewhere due to higher nutrient accumulation and shallower water depth (Yang *et al.*, 2011). Previous studies estimated that the total CH₄ emission from lakes in Eastern China (total lake area 21053 km², Yang *et al.*, 2011) is 0.23 Tg year⁻¹ (Chen *et al.*, 2013), giving an

average flux density of $10.92 \text{ g m}^{-2} \text{ year}^{-1}$. Averaged diffusion CH_4 flux at macrophyte zone (Dongtaihu Bay and East Zone:) and eutrophic zones (Meiliang Bay and Northwest Zone) of Lake Taihu were 1.16 and $0.82 \text{ g m}^{-2} \text{ year}^{-1}$, respectively. Considering the ebullition emission at eutrophic zone and macrophyte zone (Figure 8), the total flux were 2.26 and $2.78 \text{ g m}^{-2} \text{ year}^{-1}$, respectively, which were still lower than reported value. The large discrepancy may have been contributed by two factors. First, previous studies mainly focus on lake littoral zones where vegetation is abundant and the flux is high (Xing *et al.*, 2005; Wang *et al.*, 2006; Chen *et al.*, 2009). Second, the majority of the field measurements used by the synthesis study of Chen *et al.* (2013) were conducted during the warm season. Consistent with Natchimuthu *et al.* (2015), the high temporal and spatial variabilities documented here (Figures 3 and 4) emphasize the importance of year-long and spatially distributed sampling in order to achieve unbiased results.

4.6 CH_4 flux comparison based on different diffusivity formulations

The diffusion CH_4 flux reported here was based on the wind-dependent gas transfer coefficient formula described by Cole *et al.* (1998). We also compared the flux computed with several new models for the transfer coefficient. Although these models deploy empirical coefficients, they all calculate k as the sum of wind shear-driven and (waterside) convection-driven contributions. In our application, the shear-driven part was evaluated with either measured wind speed or (air side) friction velocity, and the convection part was evaluated with the heat flux in the water column which was calculated as the residual of the surface energy balance. On average, the contribution of waterside convection was less than

5%. The result is consistent with previous studies showing that gas transfer in large lakes is driven primarily by wind shear (Read *et al.*, 2012). The annual mean CH₄ diffusion fluxes based on different diffusivity formulations were 0.092 mmol m⁻² d⁻¹ (Cole *et al.*, 1998), 0.103 mmol m⁻² d⁻¹ (Read *et al.*, 2012), 0.080 mmol m⁻² d⁻¹ (Heiskanen *et al.*, 2014), and 0.093 mmol m⁻² d⁻¹ (Podgrajsek *et al.*, 2015; Supplementary Figure S7). The good agreement suggests that even though the model given by Cole *et al.* (1998) uses wind as the only input variable, it may have captured implicitly the convection effect because its model coefficients were calibrated against diffusion flux data.

5 Conclusions

The field measurement in Lake Taihu over a three year period showed that the highest CH₄ fluxes occurred in Dongtaihu Bay, a zone dominated by submerged macrophytes, and in the highly eutrophic Northwest Zone. Spatially, 78% of the flux variations were explained by water clarity, dissolved oxygen concentration, water depth and NDVI.

In the Northwest Zone, which receives the majority (35%) of river nutrient discharge to the lake, neither of the water quality indices (chlorophyll concentration, dissolved oxygen concentration) nor water temperature were correlated with the observed temporal variability in the diffusion CH₄ flux; instead, the variability in the diffusion CH₄ flux was positively correlated with NDVI, a proxy measure of algal biomass. In comparison, the temporal variability in the diffusion flux in the East Zone showed high correlation with water temperature ($R = 0.81, p < 0.01$).

666 A comparison of the flux measured with the transfer coefficient method and that measured
667 with the micrometeorological methods showed that the ebullition contribution to the total flux
668 was $71\% \pm 6\%$ in the eutrophic zone (Meiliang Bay) and to $49\% \pm 8\%$ in the submerged
669 macrophyte zone (the East Zone). The large uncertainty, probably caused by the episodic
670 nature of ebullition, emphasizes the need for more frequent measurements.

671

672 The annual whole-lake mean diffusion flux was $0.092 \pm 0.052 \text{ mmol m}^{-2} \text{ d}^{-1}$, which was an
673 order of magnitude greater than the value suggested by the flux-lake size relationship found
674 in the literature. However, the CH_4 flux in this large and shallow eutrophic lake may be much
675 lower than that reported in a synthesis study by Chen *et al.* (2013) for lakes in Eastern China.
676

677 **Acknowledgements**

678 The research was funded jointly by the National Natural Science Foundation of China (Grant
679 41575147, 41475141, and 41505005), the Priority Academic Program Development of
680 Jiangsu Higher Education Institutions (PARD), the Ministry of Education of China (Grant
681 PCSIRT), and the Natural Science Foundation of Jiangsu Province, China (Grant
682 BK20150900). The first author acknowledges the support Innovation Project for Graduate
683 Students of Jiangsu Province (Grant KYZZ15_0246). We thank the editor Dr. Ankur Desai
684 and the journal reviewers whose detailed comments have improved this paper. Some
685 micro-meteorological data and flux-gradient CH₄ flux be accessed through the Internet at
686 <http://yncenter.sites.yale.edu/publications>. Other CH₄ flux and ancillary data can be obtained
687 by contacting the corresponding author.

References

- Bastviken, D., J. Cole, M. Pace, and L. Tranvik (2004), Methane emissions from lakes: Dependence of lake characteristics, two regional assessments, and a global estimate, *Global Biogeochem. Cycles*, 18(4), GB4009, doi:10.1029/2004gb002238.
- Bastviken, D., J. J. Cole, M. L. Pace, and M. C. Van de Bogert (2008), Fates of methane from different lake habitats: Connecting whole-lake budgets and CH₄ emissions, *J. Geophys. Res.*, 113, G02024, doi:10.1029/2007jg000608.
- Bastviken, D., L. J. Tranvik, J. A. Downing, P. M. Crill, and A. Enrich-Prast (2011), Freshwater methane emissions offset the continental carbon sink, *Science*, 331(6013), 50-50.
- Bouchard, V., S. D. Frey, J. M. Gilbert, and S. E. Reed (2007), Effects of macrophyte functional group richness on emergent freshwater wetland functions, *Ecology*, 88(11), 2903-2914.
- Bridgham, S. D., H. Cadillo-Quiroz, J. K. Keller, and Q. Zhuang (2013), Methane emissions from wetlands: biogeochemical, microbial, and modeling perspectives from local to global scales, *Global Change Biol.*, 19(5), 1325-1346, doi:10.1111/gcb.12131.
- Carmichael, M. J., E. S. Bernhardt, S. L. Bräuer, and W. K. Smith (2014), The role of vegetation in methane flux to the atmosphere: should vegetation be included as a distinct category in the global methane budget?, *Biogeochemistry*, 119(1-3), 1-24, doi:10.1007/s10533-014-9974-1.
- Chen, H., N. Wu, S. Yao, Y. Gao, D. Zhu, Y. Wang, W. Xiong, and X. Yuan (2009), High methane emissions from a littoral zone on the Qinghai-Tibetan Plateau, *Atmos. Environ.*, 43(32), 4995-5000, doi:10.1016/j.atmosenv.2009.07.001.
- Chen, H., et al. (2013), Methane emissions from rice paddies natural wetlands, and lakes in China: synthesis and new estimate, *Global Change Biol.*, 19(1), 19-32, doi:10.1111/gcb.12034.
- Cho, H., and D. Lu (2010), A water-depth correction algorithm for submerged vegetation spectra, *Remote Sensing Letters*, 1(1), 29-35.
- Cole, J. J., and N. F. Caraco (1998), Atmospheric exchange of carbon dioxide in a low-wind oligotrophic lake measured by the addition of SF₆, *Limnol. Oceanogr.*, 43(4), 647-656.
- Crawford, J. T., E. H. Stanley, S. A. Spawn, J. C. Finlay, L. C. Loken, and R. G. Striegl (2014), Ebullitive methane emissions from oxygenated wetland streams, *Global Change Biol.*, 20(11), 3408-3422, doi:10.1111/gcb.12614.
- Crawford, J. T., R. G. Striegl, K. P. Wickland, M. M. Dornblaser, and E. H. Stanley (2013), Emissions of carbon dioxide and methane from a headwater stream network of interior Alaska, *J. Geophys. Res. Biogeosci.*, 118, 482-494, doi:10.1002/jgrg.20034.

- Davidson, T. A., J. Audet, J. C. Svenning, T. L. Lauridsen, M. Søndergaard, F. Landkildehus, S. E. Larsen, and E. Jeppesen (2015), Eutrophication effects on greenhouse gas fluxes from shallow lake mesocosms override those of climate warming, *Global Change Biol.*, 21(12), 4449-4463.
- DelSontro, T., M. J. Kunz, T. Kempter, A. Wuest, B. Wehrli, and D. B. Senn (2011), Spatial heterogeneity of methane ebullition in a large tropical reservoir, *Environ. Sci. Technol.*, 45(23), 9866-9873, doi:10.1021/es2005545.
- Deng, B., S. Liu, W. Xiao, W. Wang, J. Jin, and X. Lee (2013), Evaluation of the CLM4 lake model at a large and shallow freshwater lake, *J. Hydrometeorol.*, 14(2), 636-649.
- Ding, W. X., Z. C. Cai, and H. Tsuruta (2005), Plant species effects on methane emissions from freshwater marshes, *Atmos. Environ.*, 39(18), 3199-3207, doi:10.1016/j.atmosenv.2005.02.022.
- Fritz, C., V. A. Pancotto, J. T. Elzenga, E. J. Visser, A. P. Grootjans, A. Pol, R. Iturraspe, J. G. Roelofs, and A. J. Smolders (2011), Zero methane emission bogs: extreme rhizosphere oxygenation by cushion plants in Patagonia, *New. Phytol.*, 190(2), 398-408, doi:10.1111/j.1469-8137.2010.03604.x.
- Furlanetto, L. M., C. C. Marinho, C. Palma-Silva, E. F. Albertoni, M. P. Figueiredo-Barros, and F. d. A. Esteves (2012), Methane levels in shallow subtropical lake sediments: Dependence on the trophic status of the lake and allochthonous input, *Limnologica*, 42(2), 151-155, doi:10.1016/j.limno.2011.09.009.
- Gogo, S., C. Guimbaud, F. Laggoun-Défarge, V. Catoire, and C. Robert (2011), In situ quantification of CH₄ bubbling events from a peat soil using a new infrared laser spectrometer, *J. Soil. Sediment.*, 11(4), 545-551, doi:10.1007/s11368-011-0338-3.
- Gu, X., S. Zhang, X. Bai, W. Hu, Y. Hu, and X. Wang (2005), Evolution of community structure of aquatic macrophytes in East Taihu Lake and its wetlands (in Chinese), *Acta Ecologica Sinica*, 25(7), 1543-1548.
- Heiskanen, J., I. Mammarella, S. Haapanala, J. Pumpanen, T. Vesala, S. MacIntyre, A. Ojala (2014), Effects of cooling and internal wave motions on gas transfer coefficients in a boreal lake, *Tellus B*, 66, doi:10.3402/tellusb.v66.22827.
- Holgerson, M. A., and P. A. Raymond (2016), Large contribution to inland water CO₂ and CH₄ emissions from very small ponds, *Nat. Geosci.*, 9, 222-226.
- Holzapfel-Pschorn, A., R. Conrad, and W. Seiler (1986), Effects of vegetation on the emission of methane from submerged paddy soil, *Plant. Soil.*, 92, 223-233.
- Hu, Q. W., J. Y. Cai, B. Yao, Q. Wu, Y. Q. Wang, and X. L. Xu (2015), Plant-mediated methane and nitrous oxide fluxes from a carex meadow in Poyang Lake during drawdown periods, *Plant Soil*, 40(1), 367-380, doi:10.1007/s11104-015-2733-9.
- Hu, W. P., S. E. Jørgensen, F. B. Zhang, Y. G. Chen, Z. X. Hu, and L. Y. Yang (2011), A model on the

carbon cycling in Lake Taihu, China, *Ecol. Model.*, 222(16), 2973-2991,
doi:10.1016/j.ecolmodel.2011.04.018.

Hu, Z. H., Q. Xiao, J. Yang, W. Xiao, W. Wang, S. Liu, X. Lee (2015), Temporal dynamics and drivers of
ecosystem metabolism in a large subtropical shallow lake (Lake Taihu), *Int. J. Environ. Res. Public Health*,
12(4), 3691 - 3706.

Huttunen, J. T., J. Alm, A. Liikanen, S. Juutinen, T. Larmola, T. Hammar, J. Silvola, and P. J. Martikainen
(2003), Fluxes of methane, carbon dioxide and nitrous oxide in boreal lakes and potential anthropogenic
effects on the aquatic greenhouse gas emissions, *Chemosphere*, 52(3), 609-621,
doi:10.1016/s0045-6535(03)00243-1.

Johnson, K. M., J. E. Hughes, P. L. Donaghay, J. M. Sieburth (1990), Bottle-calibration static head space
method for the determination of methane dissolved in Seawater, *Anal. Chem.*, 62, 2408 - 2412.

Joyce, J., and P. W. Jewell (2003), Physical controls on methane ebullition from reservoirs and lakes,
Environ. Eng. Geosci., 9(2), 167-178.

Lee, X., *et al.* (2014), The Taihu Eddy Flux Network: an observational program on energy, water and
greenhouse gas fluxes of a large freshwater lake, *B. Am. Meteorol. Soc.*, 95(10), 1583-1594,
doi:10.1175/bams-d-13-00136.1.

Lee, X., and W. J. Massman (2011), A perspective on thirty years of the Webb, Pearman and Leuning
density corrections, *Boundary Layer Meteorol.*, 139(1), 37-59.

MacIntyre, S., A. Jonsson, M. Jansson, J. Aberg, D. E. Turney, and S. D. Miller (2010), Buoyancy flux,
turbulence, and the gas transfer coefficient in a stratified lake, *Geophys. Res. Lett.*, 37, L24604,
doi:10.1029/2010GL044164.

Maeck, A., T. Delsontro, D. F. McGinnis, H. Fischer, S. Flury, M. Schmidt, P. Fietzek, and A. Lorke (2013),
Sediment trapping by dams creates methane emission hot spots, *Environ. Sci. Technol.*, 47(15), 8130-8137,
doi:10.1021/es4003907.

Marotta, H., L. Pinho, C. Gudas, D. Bastviken, L. J. Tranvik, and A. Enrich-Prast (2014), Greenhouse gas
production in low-latitude lake sediments responds strongly to warming, *Nat. Clim. Change*, 4(6), 467-470.

Manns ,H., A. Berg (2013), Importance of soil organic carbon on surface soil water content
variability among agricultural fields, *J. Hydrol.*, 516, 297-303.

Musenze, R. S., A. Grinham, U. Werner, D. Gale, K. Sturm, J. Udy, and Z. Yuan (2014), Assessing the
spatial and temporal variability of diffusive methane and nitrous oxide emissions from subtropical
freshwater reservoirs, *Environ. Sci. Technol.*, 48(24), 14499-14507, doi:10.1021/es505324h.

Natchimuthu, S., I. Sundgren, M. Gålfalk, L. Klemedtsson, P. Crill, Å. Danielsson, D. Bastviken (2015),

Spatio-temporal variability of lake CH₄ fluxes and its influence on annual whole lake emission estimates, *Limnol. Oceanogr.*, doi: 10.1002/lno.10222.

Ojala, A., J. L. Bellido, T. Tulonen, P. Kankaala, and J. Huotari (2011), Carbon gas fluxes from a brown-water and a clear-water lake in the boreal zone during a summer with extreme rain events, *Limnol. Oceanogr.*, 56(1), 61-76.

Palma-Silva, C., C. C. Marinho, E. F. Albertoni, I. B. Giacomini, M. P. Figueiredo Barros, L. M. Furlanetto, C. R. T. Trindade, and F. d. A. Esteves (2013), Methane emissions in two small shallow neotropical lakes: The role of temperature and trophic level, *Atmos. Environ.*, 81, 373-379, doi:10.1016/j.atmosenv.2013.09.029.

Peltola, O., I. Mammarella, S. Haapanala, G. Burba, and T. Vesala (2013), Field intercomparison of four methane gas analyzers suitable for eddy covariance flux measurements, *Biogeosciences*, 10(6), 3749-3765, doi:10.5194/bg-10-3749-2013.

Podgrajsek, E., E. Sahlée, and A. Rutgersson (2014), Diurnal cycle of lake methane flux, *J. Geophys. Res. Biogeosci.*, 119(3), doi:10.1002/2013jg002327.

Podgrajsek, E., E. Sahlée, and A. Rutgersson (2015), Diel cycle of lake-air CO₂ flux from a shallow lake and the impact of waterside convection on the transfer velocity, *J. Geophys. Res. Biogeosci.*, 120(1), 29-38, doi:10.1002/2014jg002781.

Qin, B., P. Xu, Q. Wu, L. Luo, and Y. Zhang (2007), Environmental issues of Lake Taihu, China, *Hydrobiologia*, 581(1), 3-14, doi:10.1007/s10750-006-0521-5.

Rasilo, T., Y. T. Prairie, and P. A. del Giorgio (2015), Large-scale patterns in summer diffusive CH₄ fluxes across boreal lakes, and contribution to diffusive C emissions, *Global Change Biol.*, 21(3), 1124-1139, doi:10.1111/gcb.12741.

Read, J. S., *et al.* (2012), Lake-size dependency of wind shear and convection as controls on gas exchange, *Geophys. Res. Lett.*, 39(9), doi:10.1029/2012gl051886.

Sawaya, K., L. Olmanson, N. Heinert, P. Brezonik, and M. Bauer (2003), Extending satellite remote sensing to local scales: land and water resource monitoring using high-resolution imagery, *Remote Sensing of Environment*, 88, 144-156.

Schubert, C. J., T. Diem, and W. Eugster (2012), Methane emissions from a small wind shielded lake determined by eddy covariance, flux chambers, anchored funnels, and boundary model calculations: a comparison, *Environ. Sci. Technol.*, 46(8), 4515- 4522, doi:10.1021/es203465x.

Segers, R. (1998), Methane production and methane consumption: a review of processes underlying wetland methane fluxes, *Biogeochemistry*, 48(1), 23-51.

- Sorrell, B., and F. Dromgoole (1987), Oxygen transport in the submerged freshwater macrophyte *Egeria densa* Planch. I. oxygen production, storage and release, *Aquat. Bot.*, 28(1), 63-80.
- Striegl, R. G., M. M. Dornblaser, C. P. McDonald, J. R. Rover, and E. G. Stets (2012), Carbon dioxide and methane emissions from the Yukon River system, *Global Biogeochem. Cycles*, 26, GB0E05, doi:10.1029/2012GB004306.
- Sturm, K., Z. Yuan, B. Gibbes, U. Werner, and A. Grinham (2014), Methane and nitrous oxide sources and emissions in a subtropical freshwater reservoir, South East Queensland, Australia, *Biogeosciences*, 11(18), 5245-5258, doi:10.5194/bg-11-5245-2014.
- Verpoorter, C., T. Kutser, D. A. Seekell, and L. J. Tranvik (2014), A global inventory of lakes based on high-resolution satellite imagery, *Geophys. Res. Lett.*, 41(18), 6396-6402.
- Wang, H., J. Lu, W. Wang, L. Yang, and C. Yin (2006), Methane fluxes from the littoral zone of hypereutrophic Taihu Lake, China, *J. Geophys. Res.*, 111, D17109, doi:10.1029/2005jd006864.
- Wang, W., *et al.* (2014), Temporal and spatial variations in radiation and energy balance across a large freshwater lake in China, *J. Hydrol.*, 511, 811-824, doi:10.1016/j.jhydrol.2014.02.012.
- Webb, E. K., G. I. Pearman, and R. Leuning (1980), Correction of flux measurements for density effects due to heat and water vapour transfer, *Q. J. Roy. Meteor. Soc.*, 106(447), 85-100.
- Wik, M., P. M. Crill, D. Bastviken, Å. Danielsson, and E. Norbäck (2011), Bubbles trapped in arctic lake ice: Potential implications for methane emissions, *J. Geophys. Res.*, 116, G03044, doi:10.1029/2011JG001761.
- Wik, M., P. M. Crill, R. K. Varner, and D. Bastviken (2013), Multiyear measurements of ebullitive methane flux from three subarctic lakes, *J. Geophys. Res. Biogeosci.*, 118, 1307-1321, doi:10.1002/jgrg.20103.
- Wik, M., R. K. Varner, K. W. Anthony, S. MacIntyre and D. Bastviken (2016), Climate-sensitive northern lakes and ponds are critical components of methane release, *Nat. Geosci.*, 9, 99-106.
- Xiao, W., S. Liu, W. Wang, D. Yang, J. Xu, C. Cao, H. Li, X. Lee (2013) Transfer coefficients of momentum, heat and water vapour in the atmospheric surface layer of a large freshwater lake, *Boundary Layer Meteorol.*, 148, 479-494, doi:10.1007/s10546-013-9827-9.
- Xiao, W., *et al.* (2014), A flux-gradient system for simultaneous measurement of the CH₄, CO₂, and H₂O fluxes at a lake-air interface, *Environ. Sci. Technol.*, 48(24), 14490-14498, doi:10.1021/es5033713.
- Xing, Y., P. Xie, H. Yang, L. Ni, Y. Wang, and K. Rong (2005), Methane and carbon dioxide fluxes from a shallow hypereutrophic subtropical Lake in China, *Atmos. Environ.*, 39(30), 5532-5540, doi:10.1016/j.atmosenv.2005.06.010.

907 Yang, H., P. Xie, L. Ni, and R. J. Flower (2011), Underestimation of CH₄ emission from freshwater lakes
908 in China, *Environ. Sci. Technol.*, 45(10), 4203-4204, doi:10.1021/es2010336.
909
910 Zhai, S., W. Hu, and Z. Zhu (2010), Ecological impacts of water transfers on Lake Taihu from the Yangtze
911 River, China, *Ecol. Eng.*, 36(4), 406-420, doi:10.1016/j.ecoleng.2009.11.007.
912

List of Figure Captions

Figure 1. A Landsat image of Lake Taihu showing the location of spatial sampling sites and the seven biological zones: red dots, spatial sampling sites; red crosses, lake micrometeorological sites; blue lines, inflow rivers; green lines, outflow rivers; red lines, rivers with reversible flow. Purple and brown areas represent cities and green areas indicate vegetation. The red vertical bars indicate mean wind speed at the 10-m height above the water surface at five micrometeorological sites: 2.96 (MLW), 4.51 (DPK), 4.45 (BFG), 4.48 (XLS), and 4.66 m s^{-1} (PTS). The yellow vertical bars indicate mean water temperature at the 20-cm depth: 17.94 (MLW), 17.54 (DPK), 17.84 (BFG), 17.59 (XLS), and 17.69 $^{\circ}\text{C}$ (PTS). Two of the micrometeorological sites (MLW and BFG) were equipped with CH_4 flux instruments.

Figure 2: Mean spatial variation of surface water properties and water depth across Lake Taihu, (a) Normalized Difference in Vegetation Index, (b) dissolved oxygen (mg L^{-1}), (c) pH, (d) Chlorophyll a concentration ($\mu\text{g L}^{-1}$), (e) clarity (m), and (f) water depth (m).

Figure 3: Temporal variation of the CH_4 diffusion flux determined with the transfer coefficient method at the five lake observation sites (MLW, BFG, DPK, XLS, and PTS) where frequent water sampling took place. Their locations are shown in Figure 1. Time series of CH_4 concentration in the surface water and wind speed are given in Supplementary Figures S4 and S5, respectively.

Figure 4: Spatial variation of the CH₄ diffusion flux on days of whole-lake sampling in (a) spring, (b) summer, (c) autumn, and (d) winter. Data are mean values of three years (2012, 2013 and 2014).

Figure 5: Spatial variation of the mean CH₄ diffusion flux from February 2012 to November 2014.

Figure 6. Linear correlation of the whole-lake mean CH₄ diffusion and the total flux against water temperature. Diffusion flux was measured by the transfer coefficient method, and total flux was extrapolated from the micrometeorological flux measurement (see Methods). Each data point represents one lake survey. Parameter bounds on the linear regression coefficients are 95% confidence intervals.

Figure 7. Spatial correlation of the mean CH₄ diffusion flux against the (a) mean NDVI (Normalized Difference in Vegetation Index), (b) mean water depth, (c) mean pH, (d) mean water clarity. Each data point represents the 2012-2014 mean value at one spatial sampling site. Parameter bounds on the regression coefficients are 95% confidence limits.

Figure 8: Comparison of the diffusion CH₄ flux measured with the transfer coefficient method and the total flux measured with the flux-gradient method at the MLW site (a), and with the eddy covariance method at the BFG site (b). Parameter bounds on the regression coefficients are 95% confidence limits.

957 **Table 1.** Liner regression equation between diffusion CH₄ flux (y, mmol m⁻² d⁻¹) and
 958 dissolved CH₄ concentration (in parentheses: y, nmol L⁻¹) and water temperature (x, °C) in
 959 the seven lake zones. The total number of observations is 12, representing seasonal samplings
 960 between 2012 and 2014, for all the regression relations shown.

Zone	Regression equation		
Meiliang Bay	$y = 0.005x - 0.004$	$R^2 = 0.53$	$p < 0.01$
	$(y = 4.62x - 4.96$	$R^2 = 0.31$	$p = 0.06)$
Gonghu Bay	$y = 0.005x - 0.025$	$R^2 = 0.47$	$p < 0.05$
	$(y = 4.75x - 27.39$	$R^2 = 0.20$	$p = 0.14)$
East Zone	$y = 0.013x - 0.055$	$R^2 = 0.66$	$p < 0.01$
	$(y = 10.23x - 21.57$	$R^2 = 0.36$	$p = 0.04)$
Dongtaihu Bay	$y = 0.018x - 0.095$	$R^2 = 0.60$	$p < 0.01$
	$(y = 16.46x - 71.57$	$R^2 = 0.38$	$p = 0.03)$
Southwest Zone	$y = 0.004x - 0.033$	$R^2 = 0.07$	$p = 0.40$
	$(y = -1.92x + 69.29$	$R^2 = 0.02$	$p = 0.65)$
Northwest Zone	$y = -0.013x + 0.420$	$R^2 = 0.01$	$p = 0.74$
	$(y = -9.98x + 341.14$	$R^2 = 0.25$	$p = 0.01)$
Central Zone	$y = 0.002x - 0.010$	$R^2 = 0.26$	$p = 0.09$
	$(y = 1.62x + 4.18$	$R^2 = 0.05$	$p = 0.48)$
Whole lake	$y = 0.005x + 0.008$	$R^2 = 0.58$	$p < 0.01$

961

Table 2. Spatial Pearson correlation of the mean CH₄ flux against mean water quality indices:

DO, dissolved oxygen concentration; Chl-a, chlorophyll a concentration; Spc, specific
 conductance; ORP, oxidation reduction potential; NTU, turbidity; Depth, water depth; Clarity,
 water clarity. All sites: data acquired at all the spatial sampling sites; Open water: excluding
 sites in the East Zone and Dongtaihu Bay.

	DO	Chl-a	Spc	ORP	pH	NTU	Depth	Clarity
All sites	-0.43*	-0.06	0.21	0.05	-0.53**	-0.50**	-0.58**	0.60**
Open water	-0.82**	0.49*	0.61**	0.12	-0.70**	-0.38	-0.47*	0.13

*, ** Correlation is significant at the 0.05, and 0.01 level, respectively.

Table 3. The annual mean diffusion CH₄ flux in the seven zones and in the whole lake from 2012 to 2014. For the Southwest Zone and the Northwest Zone, their annual mean diffusion flux was computed as the average of the 12 seasonal surveys, and the variability range is \pm one standard deviation of the 12 samples. For the other zones, the annual mean diffusion flux was the average of the daily flux from January 1, 2012 to December 31, 2014 obtained from the linear regression with water temperature, and the standard deviation was determined with a Monte Carlo method. The diffusion flux in parentheses was estimated with an exponential regression model.

Zones	Surface area (km ²)	Diffusion CH ₄ flux (mmol m ⁻² d ⁻¹)	
		Mean	Standard deviation
Meiliang Bay	100	0.088 (0.084)	0.031
Gonghu Bay	215.6	0.064 (0.059)	0.055
East Zone	316.4	0.167 (0.170)	0.062
Dongtaihu Bay	131	0.227 (0.220)	0.101
Southwest Zone	443.2	0.039	0.036
Northwest Zone	394.1	0.191	0.117
Central Zone	737.5	0.025 (0.022)	0.015
Whole lake	2338	0.092 (0.090)	0.052

Figure 1. A Landsat image of Lake Taihu showing the location of spatial sampling sites and

the seven biological zones: red dots, spatial sampling sites; red crosses, lake

micrometeorological sites; blue lines, inflow rivers; green lines, outflow rivers; red lines,

rivers with reversible flow. Purple and brown areas represent cities and green areas indicate

vegetation. The red vertical bars indicate mean wind speed at the 10-m height above the

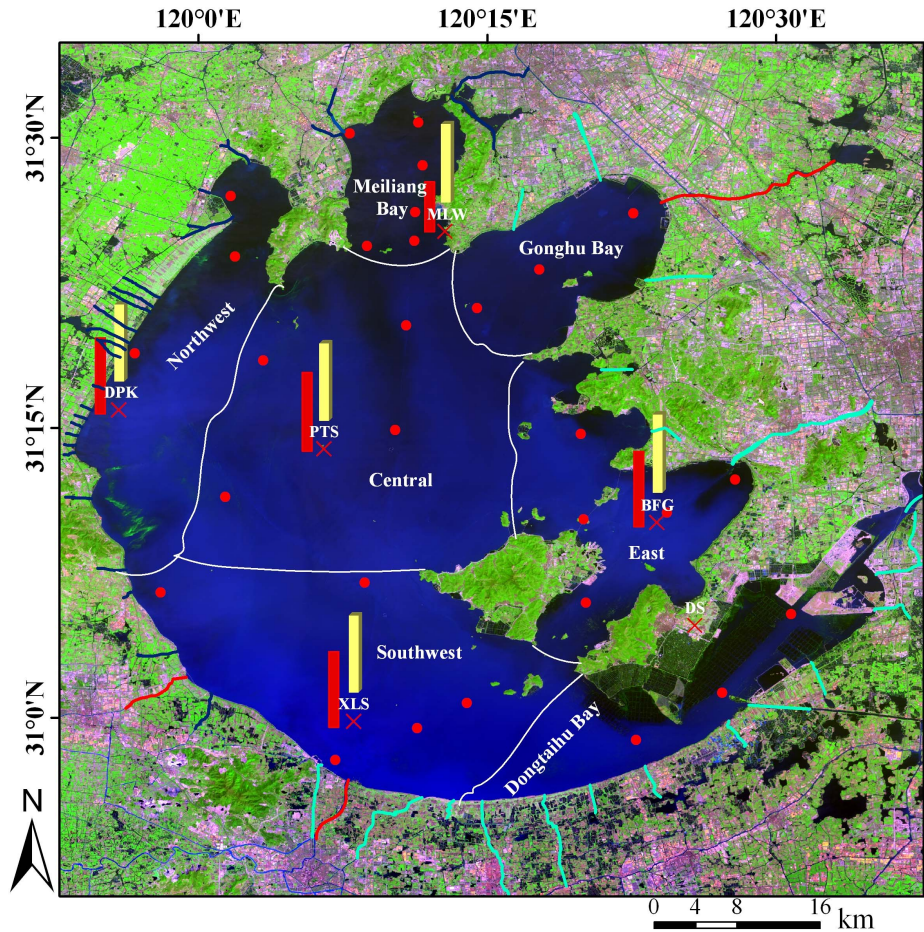
water surface at five micrometeorological sites: 2.96 (MLW), 4.51 (DPK), 4.45 (BFG), 4.48

(XLS), and 4.66 m s^{-1} (PTS). The yellow vertical bars indicate mean water temperature at the

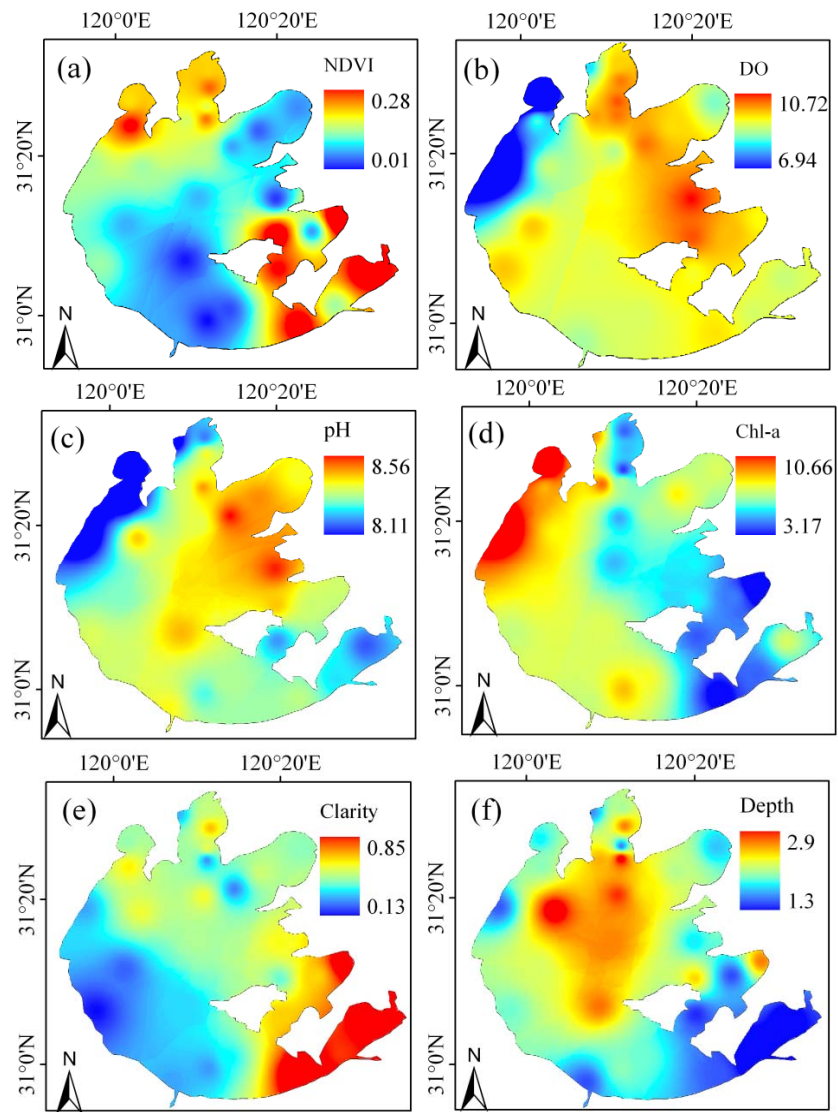
20-cm depth: 17.94 (MLW), 17.54 (DPK), 17.84 (BFG), 17.59 (XLS), and 17.69 $^{\circ}\text{C}$ (PTS).

Two of the micrometeorological sites (MLW and BFG) were equipped with CH_4 flux

instruments.

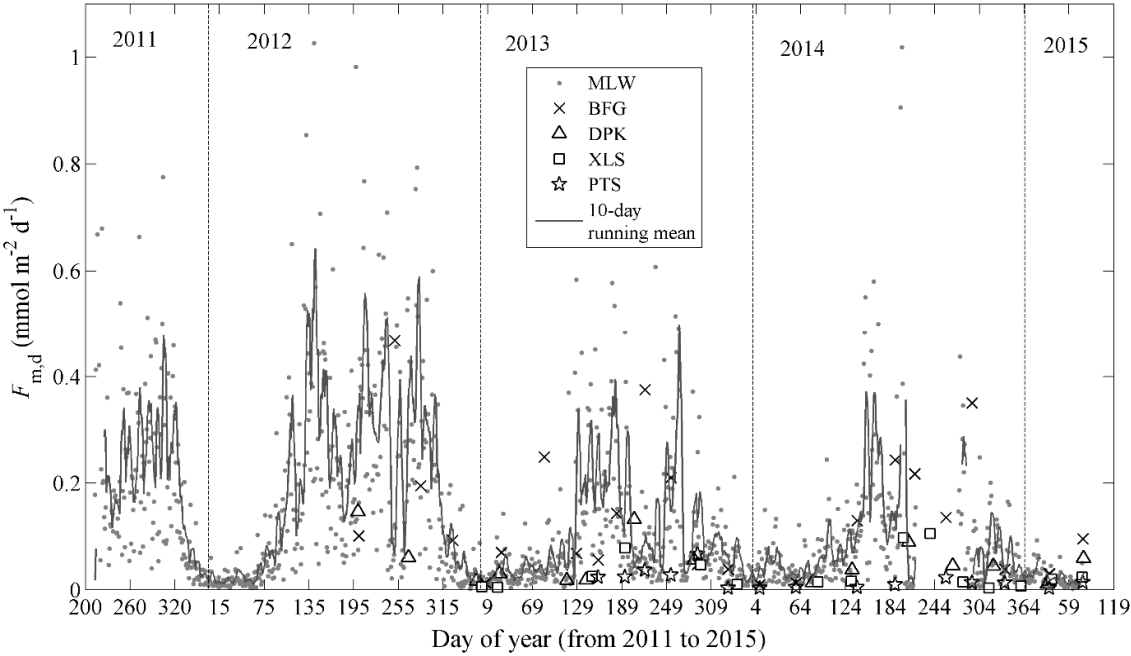


988 **Figure 2.** Mean spatial variation of surface water properties and water depth across Lake
 989 Taihu, (a) Normalized Difference in Vegetation Index, (b) dissolved oxygen (mg L^{-1}), (c) pH,
 990 (d) Chlorophyll a concentration ($\mu\text{g L}^{-1}$), (e) clarity (m), and (f) water depth (m).



991

Figure 3. Temporal variation of the CH₄ diffusion flux determined with the transfer coefficient method at the five lake observation sites (MLW, BFG, DPK, XLS, and PTS) where frequent water sampling took place. Their locations are shown in Figure 1. Time series of CH₄ concentration in the surface water and wind speed are given in Supplementary Figures S4 and S5, respectively.



999 **Figure 4.** Spatial variation of the CH₄ diffusion flux on days of whole-lake sampling in (a)
 1000 spring, (b) summer, (c) autumn, and (d) winter. Data are mean values of three years (2012,
 1001 2013 and 2014).

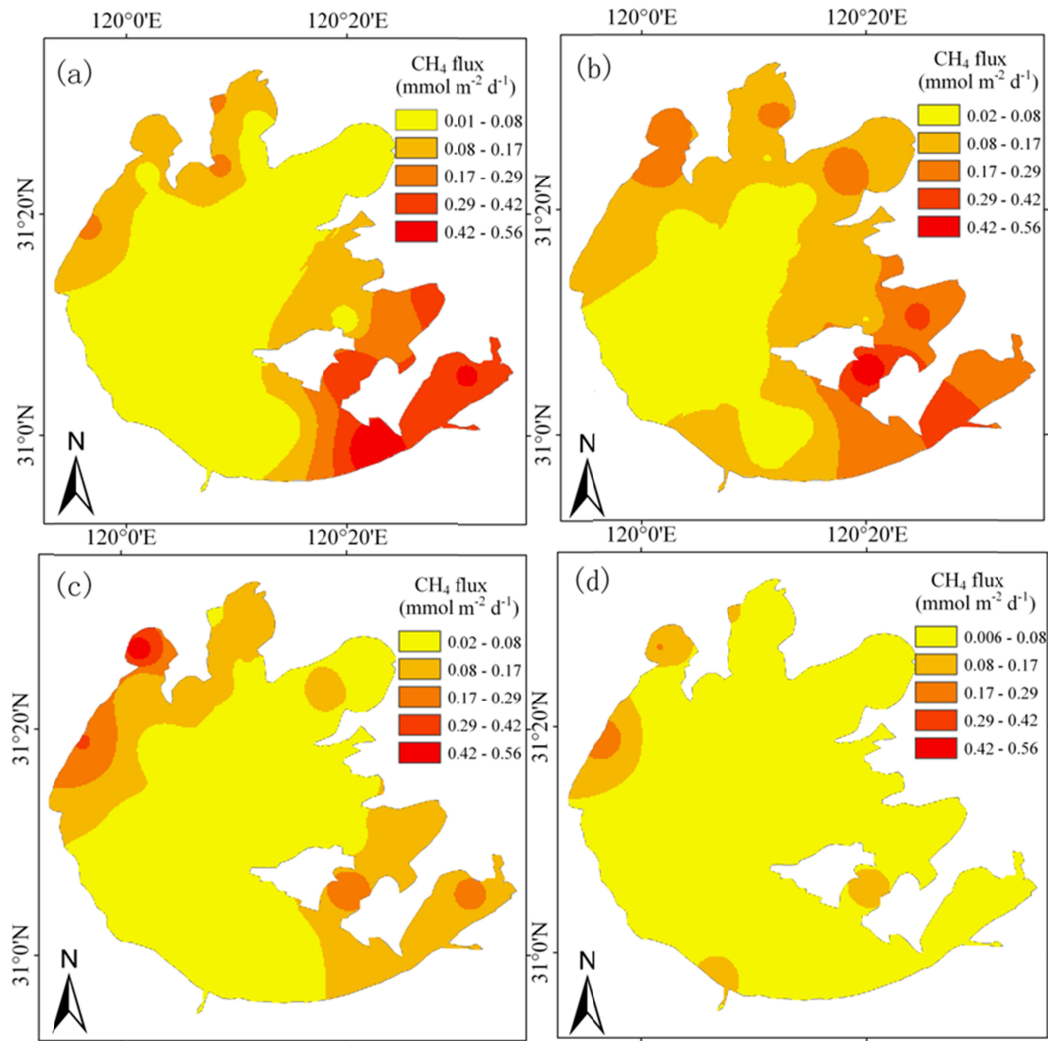


Figure 5. Spatial variation of the mean CH₄ diffusion flux from February 2012 to November 2014.

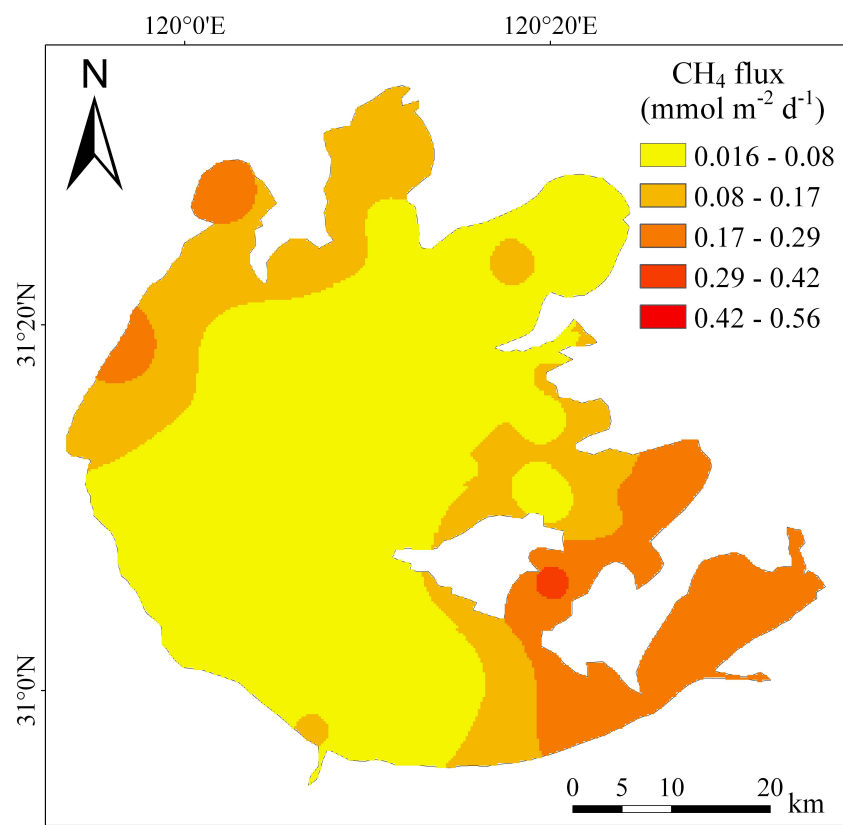
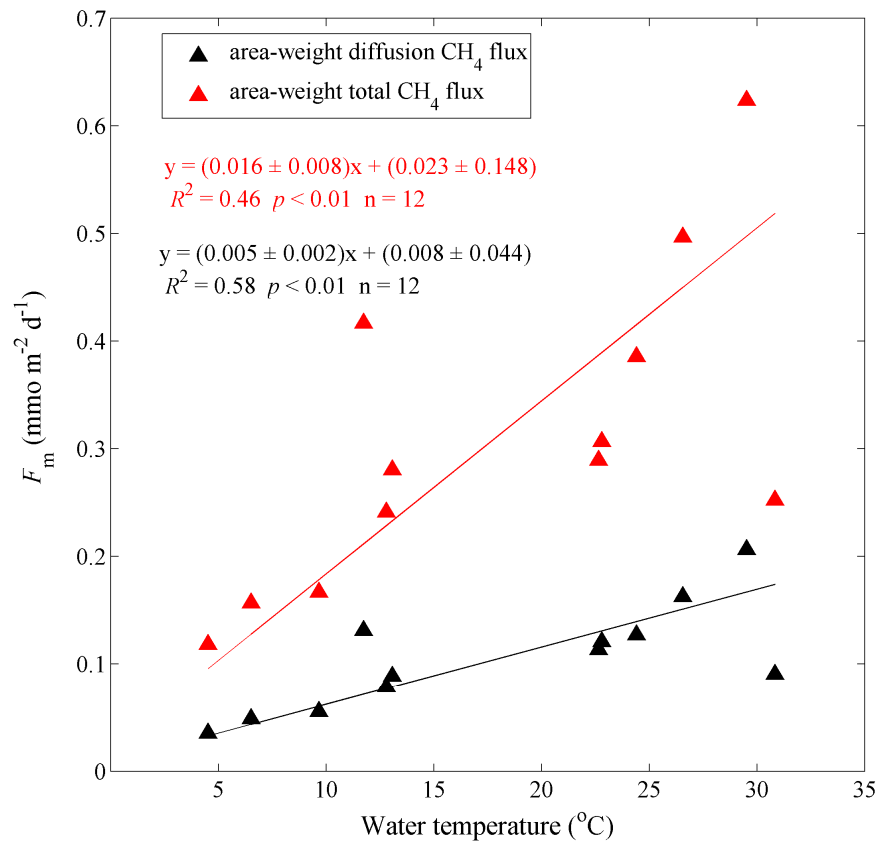
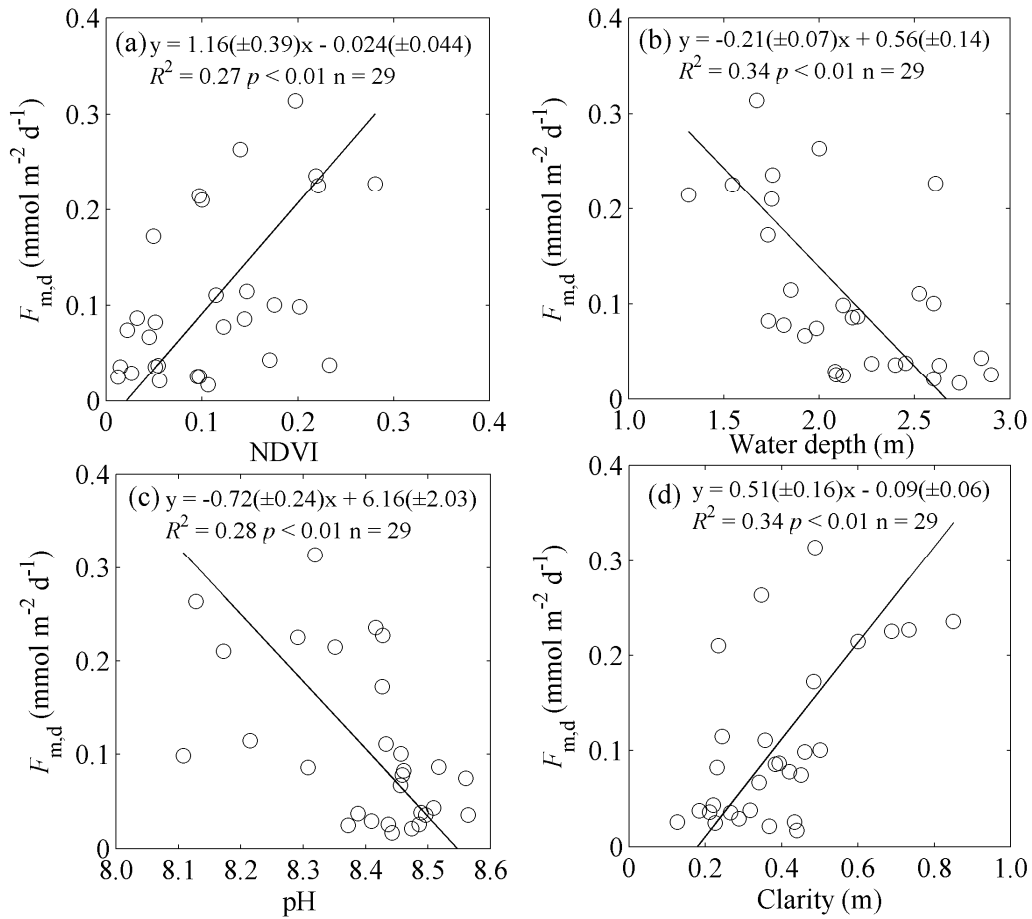


Figure 6. Linear correlation of the whole-lake mean CH₄ diffusion and the total flux against water temperature. Diffusion flux was measured by the transfer coefficient method, and total flux was extrapolated from the micrometeorological flux measurement (see Methods). Each data point represents one lake survey. Parameter bounds on the linear regression coefficients are 95% confidence intervals.



1013 **Figure 7.** Spatial correlation of the mean CH₄ diffusion flux against the (a) mean
1014 NDVI (Normalized Difference in Vegetation Index), (b) mean water depth, (c) mean
1015 pH, (d) mean water clarity. Each data point represents the 2012-2014 mean value at
1016 one spatial sampling site. Parameter bounds on the regression coefficients are 95%
1017 confidence limits.



1018

Figure 8. Comparison of the diffusion CH₄ flux measured with the transfer coefficient method and the total flux measured with the flux-gradient method at the MLW site (a), and with the eddy covariance method at the BFG site (b). Parameter bounds on the regression coefficients are 95% confidence limits.

